

The structure-tunable synthesis and magnetic properties of Fe₃O₄ nanocrystals

Yi Liu · Zhao-Fen Gao · Qingbo Sun · Yu-Ping Zeng

© Springer Science+Business Media Dordrecht 2013

Abstract Magnetite nanocrystals with tunable crystalline structures (orthorhombic and cubic) were synthesized via a simple oxidation-coprecipitation approach basing on the reaction of FeSO₄·7H₂O with C₆H₁₂N₄. The average diameter of prepared orthorhombic Fe₃O₄ nanorods were 15 nm while their lengths were approximately 150~200 nm. As-prepared cubic counterparts were composed of 10 nm sized nanoparticles. XRD, FESEM, TEM, SAED and HRTEM were then used to characterize our samples. In addition, magnetic measurements showed the saturation magnetization of orthorhombic magnetite was lower than that of cubic ones. Mössbauer spectroscopy verified the samples possessed the nature of cubic magnetite. Finally, a possible growth mechanism for orthorhombic nanorods and cubic nanoparticles was also discussed.

Keywords Orthorhombic and cubic magnetite · Oxidation-coprecipitation · Magnetism · Mössbauer spectroscopy · Nanocrystals

1 Introduction

Controllable synthesis of architectural nanocrystals (NCs) has been deemed as important issues of material science since the properties of NCs depend not only on

Y. Liu (✉)
College of Chemistry Chemical Engineering & Material Science, Zaozhuang University,
Zaozhuang 277160, People's Republic of China
e-mail: 1967liuyi@163.com

Z.-F. Gao
College of Chemistry Chemical Engineering, Shangrao Normal College,
Shangrao, 334001, People's Republic of China

Q. Sun · Y.-P. Zeng
Shanghai Institute of Ceramics, Chinese Academy of Science, 1295 Dingxi Road,
Shanghai 200050, People's Republic of China

their composition but also on their structure, phase shape, size and size distribution. As one of the most important magnetic materials, fabrications of magnetite NCs (Fe_3O_4) recently have received increasing attention for their potential applications in diverse areas such as biomedicine, high-density magnetic storage devices, spin electronics, etc [1–3]. Meanwhile, experimental routes mainly focus on reduction of hematite by CO/CO_2 or H_2 [4, 5], coprecipitation of ferrous/ferric mixed salt solutions [6], microwave plasma and ultrasound irradiation methods [7, 8], micro-emulsion processes [9] and others.

From crystallographic viewpoints, magnetite possesses many possible crystal structures such as cubic inverse spinel or perovskite-based orthorhombic [10]. More important, any small changes for crystal structure would cause large alternations in magnetic symmetry. So it is valuable in application and science to deeply understand the magnetic properties of magnetite NCs relating to special crystal structure and their mutual interactions [11]. Fewer papers, however, report about orthorhombic magnetite NCs.

Here, a novel oxidation-coprecipitation method is designed to tune crystal structure of magnetite NCs (orthorhombic or cubic) and control the morphologies. Microscopic structures and macroscopic magnetism are further characterized by XRD, FESEM, TEM, SAED, HRTEM and Mössbauer spectroscopy. The formation mechanism about different structures is simply analyzed, too.

2 Experimental

In a typical experiment, 1.12 g ferrous sulfate heptahydrate ($\text{FeSO}_4 \cdot 7\text{H}_2\text{O}$) and 0.84 g methenamine ($\text{C}_6\text{H}_{12}\text{N}_4$) were added into 40 mL distilled water until a homogeneous solution appeared. The solution was then transferred into a round bottom flask with 100 mL capacity while 40 mL different solvents were added. The above solutions were then magnetically stirred and heated at 60 °C using water bath for different time. After being filtered and washed with distilled water and ethanol for several times to eliminate impurities, the samples were finally dried in vacuum at 80 °C for 1 h.

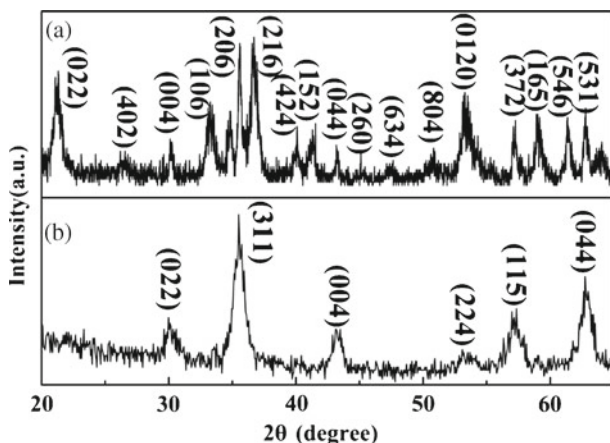
Mössbauer studies were performed on a spectrometer equipped with a low temperature setup. The initial activity of γ -ray radiation source $^{57}\text{Co}(\text{pb})$ is 25 mCi at room temperature. The isomer shifts were measured relative to metal α -Fe at 300 K. Other data were obtained from XRD, FE-SEM, (HR)TEM, SAED equipments.

3 Results and discussion

Experimental results obtained at different reaction conditions are summarized in Table 1. It could be found that the formation of Fe_3O_4 NCs is driven by kinetic rather than thermodynamic control [12]. Actually, both crystal size and shape are typically manipulated by controlling growth kinetics [13]. Phase and purity of orthorhombic and cubic magnetite products were confirmed by X-ray diffraction pattern (XRD), which is shown in Fig. 1a and b, respectively. All reflection peaks in Fig. 1a can be indexed to orthorhombic Fe_3O_4 with lattice constants $a = 11.86 \text{ \AA}$, $b = 11.84 \text{ \AA}$, $c = 16.751 \text{ \AA}$. They match well with literature results (JCPDS76-0956). XRD pattern

Table 1 Summary of experimental results on products obtained with different reaction conditions at 60 °C while FeSO₄·7H₂O and C₆H₁₂N₄ are used as reactants

No.	Time	Flask	Solvents	Product	Morphology
S1	36 h	Unsealed	80 ml H ₂ O	Orthorhombic FeOOH	Nanoflakes
S2	24 h	Sealed	80 ml H ₂ O	Orthorhombic Fe ₃ O ₄	Nanorods
S3	22 h	Sealed	40 ml H ₂ O+40 ml ethanol	Cubic Fe ₃ O ₄	Nanorods
S4	8 h	Sealed	40 ml H ₂ O+40 ml Glycol	Cubic Fe ₃ O ₄	Nanoparticles
S5	4 h	Sealed	40 ml H ₂ O+40 ml Glycol	Cubic Fe ₃ O ₄	Nanoflakes

Fig. 1 XRD patterns of products obtained in water/ethanol (a) and water/glycol (b)

of Fig. 1b can be attributed to face-centered cubic spinle structure of Fe₃O₄ with a lattice parameter of $a = 8.39 \text{ \AA}$. This value closes to reported one (JCPDS 85-1436).

FE-SEM images in Fig. 2 demonstrate the products obtained in water and ethanol solutions are nanorods with diameter of 15 nm and length of 150~200 nm while the samples from water and glycol mixed solvents are composed of nanoparticles of 10 nm. The different morphologies are further confirmed by their respective TEM pictures (Fig. 3a and b). The selective areas electron diffraction (SAED) of Fig. 3d and f showed individual Fe₃O₄ nanorod is single crystallinity and the nanoparticle is polycrystalline structures. The regular spacings of lattice planes for nanorods can be observed by high-resolution TEM (HRTEM), and are ~0.272 and 0.2326 nm (Fig. 3c). They correspond to (106) and (226) planes of orthorhombic Fe₃O₄, respectively. So nanorods are growing along [106] direction. Similarly, individual Fe₃O₄ nanoparticle owns the inter-planar spacings of ~0.298 and 0.253 nm, which respectively correspond to (311) and (220) plane of cubic structure.

Previous researches indicated that the changes in sizes of the Fe₃O₄ NCs could result in great differences of magnetic properties and magnetic shape anisotropy had no effects on cubic Fe₃O₄ NCs [14, 15]. The hysteresis loop of Fig. 4a exhibits cubic Fe₃O₄ nanoparticles have ferromagnetism with saturation magnetization (M_s), remanent magnetization (M_r) and coercivity (H_c) values of respective 3.97, 1.55 emu/g and 3863.76 Oe. These values are different from those for similar Fe₃O₄ Ncs [16–20]. Though orthorhombic Fe₃O₄ nanorods are also ferromagnetic (Fig. 4b), their M_s , M_r and H_c are lower than cubic ones and are 2.19, 0.25 emu/g and 1757.39 Oe in detail.

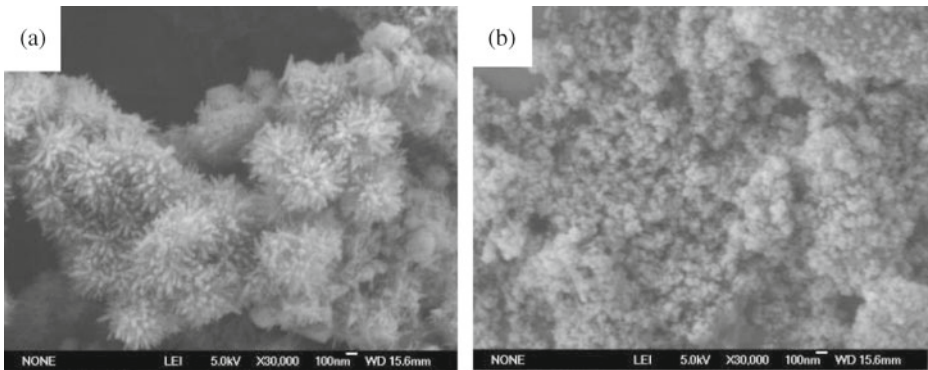


Fig. 2 FE-SEM images of orthorhombic Fe₃O₄ nanorods (a) and cubic nanoparticles (b)

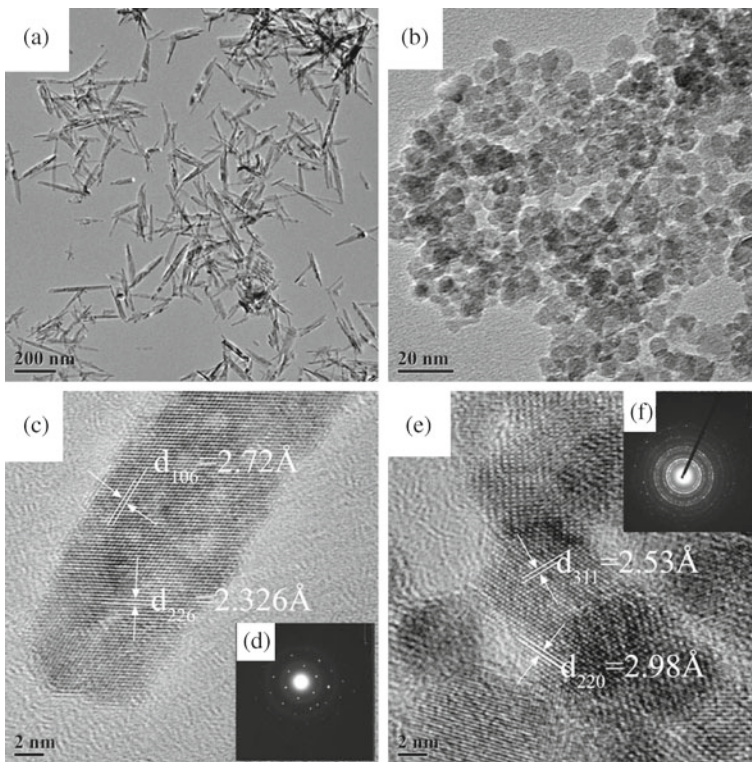
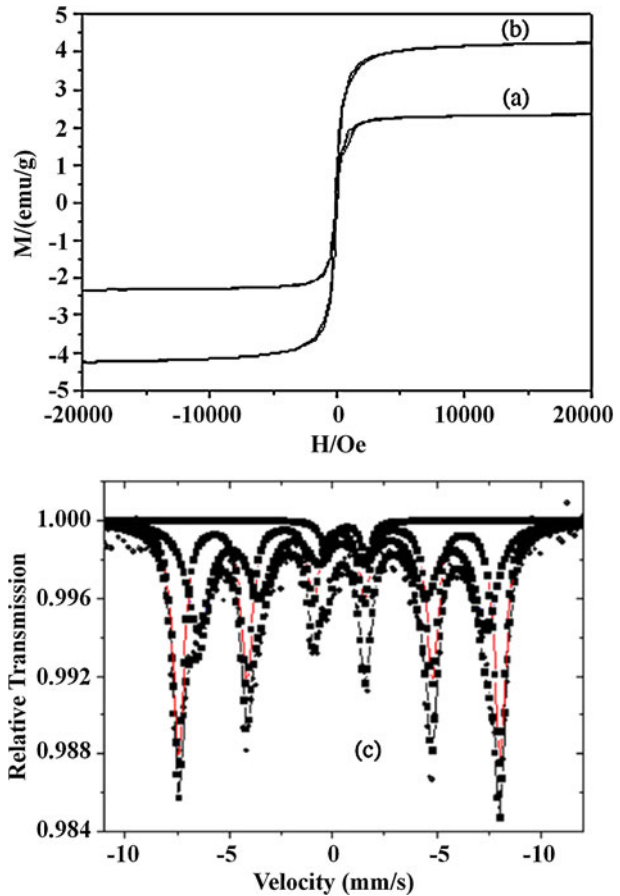


Fig. 3 (HR)TEM and SAED images of orthorhombic Fe₃O₄ nanorods (a, c and d) and cubic Fe₃O₄ nanoparticles (b, e and f)

The lower magnetization parameters for orthorhombic samples should be caused by anisotropy.

In order to confirm that the products should be Fe₃O₄ rather than γ -Fe₂O₃, Room temperature ⁵⁷Co(pb)-Mössbauer spectroscopy was then used to detect the

Fig. 4 Hysteresis loops of orthorhombic Fe_3O_4 nanorods (a) or cubic nanoparticles (b) and Mössbauer spectrum of cubic Fe_3O_4 nanoparticles at 300 K (c)



hyperfine fields of *A*- and *B*-site in two sextet splitting, which should have different values compared with that of $\gamma\text{-Fe}_2\text{O}_3$. Fig. 4c exhibits the Mössbauer spectroscopy of our nanoparticles. The hyperfine fields of the *A*- and *B*-site are 47 and 44 T, respectively. Through the large difference of hyperfine fields for two sites, it can be demonstrated that the sample is Fe_3O_4 rather than $\gamma\text{-Fe}_2\text{O}_3$ since $\gamma\text{-Fe}_2\text{O}_3$ has the similar values for the two sites. The hyperfine fields of *A*- and *B*-site for Fe_3O_4 nanoparticles are slightly different from classical spectrum of magnetite and less than that of their relative bulk materials, which is mainly attributed to the existence of collective magnetic excitation caused by the size distribution of the crystallites [21]. Therefore, our measured sample should be cubic magnetite (Fe_3O_4).

4 Conclusion

Overall orthorhombic Fe_3O_4 nanorods and cubic nanoparticles have been firstly synthesized through a novel oxidation-coprecipitation method. Experimental results confirmed their crystalline structures and magnetic properties. Although much work

is required to understand the phase transformation process, our method may be used to produce other metal oxides nanomaterials at a lower temperature.

Acknowledgements Financial support from the key scientific and technological project of Shandong Province (2009GG10002033) is greatly appreciated. The author thanks Dr. Jun Lin at Shanghai Institute of Applied Physics, Chinese Academy of Science for his helpful works in Mössbauer measurements.

References

1. Berry, C.C., Curtis, A.S.D.: *J. Phys. D* **46**, R198 (2003)
2. Zhu, J.G.: *IEEE Trans. Magn.* **29**, 195 (1993)
3. Zutic, I., Fabian, J.: *Rev. Mod. Phys.* **76**, 323 (2004)
4. Darken, L.S., Gurry, R.W.: *J. Am. Chem. Soc.* **68**, 798 (1946)
5. Osterhout, V.: In: Craik, D.S. (ed.) *Magnetic Oxides*. Wiley, New York (1975)
6. Visalakshi, G., Venkateswaran, G., Kulshreshtha, S.K., Moorphy, P.H.: *Mater. Res. Bull.* **28**, 829 (1993)
7. Vollath, D., Szabo, D.V.: *J. Mater. Res.* **12**, 2175 (1997)
8. Kumar, R.V., Kolytyn, Y., Xu, X.N., Yeshurun, Y., Gedanken, A., Felner, I.: *J. Appl. Phys.* **89**, 6324 (2001)
9. Mann, S., Sparks, H.C., Board, R.G.: *Adv. Microb. Physiol.* **31**, 125 (1990)
10. Siwach, P.K., Singh, H.K., Srivastava, O.N.: *J. Phys.: Condens. Matter.* **20**, 273201 (2008)
11. Bae, C.J., Angappane, S., Park, J.-G.: *Appl. Phys. Lett.* **91**, 102502 (2007)
12. Murphy, C.J.: *Science* **298**, 2139 (2002)
13. Gugliotti, L.A., Feldheim, D.L., Eaton, B.E.: *J. Am. Chem. Soc.* **127**, 17814 (2005)
14. Song, Q., Zhang, Z.J.: *J. Am. Chem. Soc.* **126**, 6164 (2004)
15. Cao H.Q., Wang, G.Z.: *Appl. Phys. Lett.* **92**, 013110 (2008)
16. Goya, G.F., Berquo, T.S., Fonseca, F.C.: *J. Appl. Phys.* **94**, 3520 (2003)
17. Han, D.H., Wang, J.P., Luo, H.L.: *J. Magn. Mater.* **136**, 176 (1994)
18. Wang, J., Chen, Q.W., Zeng, C., Hou, B.Y.: *Ad. Mater.* **16**, V137 (2004)
19. Xu, L.Q., Zhang, W.Q., Ding, Y.W., Peng, Y.Y., Zhang, S.Y., Yu, W.C., Qian, Y.T.: *J. Phys. Chem. B.* **108**, 10859 (2004)
20. Zhang, D.E., Zhang, X.J., Ni, X.M., Song, J.M., Zheng, H.G.: *Cryst. Growth Des.* **7**(10), 2119 (2007)
21. Borzi, R.A., Steward, S.J., Punte, G., Mercader, R.C., Mansilla, M.V., Zysler, R.D., Cabanillas, E.D.: *J. Magn. Mater.* **205**, 243 (1999)